International Journal of Medical, Medicine and Health Sciences
ISSN: 2517-9969
Vol:9, No:7, 2015

A Fuzzy Approach to Liver Tumor Segmentation with Zernike Moments

Abder-Rahman Ali, Antoine Vacavant, Manuel Grand-Brochier, Adélaïde Albouy-Kissi, Jean-Yves Boire

***Abstract*—**In this paper, we present a new segmentation approach for liver lesions in regions of interest within MRI (Magnetic Resonance Imaging). This approach, based on a two-cluster Fuzzy C-Means methodology, considers the parameter variable compactness to handle uncertainty. Fine boundaries are detected by a local recursive merging of ambiguous pixels with a sequential forward floating selection with Zernike moments. The method has been tested on both synthetic and real images. When applied on synthetic images, the proposed approach provides good performance, segmentations obtained are accurate, their shape is consistent with the ground truth, and the extracted information is reliable. The results obtained on MR images confirm such observations. Our approach allows, even for difficult cases of MR images, to extract a segmentation with good performance in terms of accuracy and shape, which implies that the geometry of the tumor is preserved for further clinical activities (such as automatic extraction of pharmaco-kinetics properties, lesion characterization, etc.).

***Keywords*—**Defuzzification, floating search, fuzzy clustering, Zernike moments.

I. Introduction

LIVER tumor segmentation is an important prerequisite for surgical interventions planning. However, the major difficulty in liver tumor segmentation is low contrasted boundaries and large variability of shape, size, and location presented by the tumor in the liver. Thus, high performance segmentation methods should be capable to deal with the high variation in shape and gray value of the liver [11]. Among image segmentation methodologies, fuzzy set theory has become increasingly attractive due to its ability to alleviate image ambiguity. Fuzzy C-Means (FCM) is one of the most well-known algorithms to partition medical images into non-overlapping and consistent regions that are homogeneous with respect to some characteristics such as texture, intensity, *etc*. However, in spite of its computational efficiency and wide spread prevalence, it does not take the spatial information into consideration, and thus may result in low robustness to noise and less accurate segmentation.

In this paper, we propose a new liver tumor segmentation approach that considers two clusters: the lesion and the surrounding tissue. FCM clustering is used due to its ability to deal with different types of uncertainty and treat overlapping clusters. This method considers both local and global information. In the FCM variational formulation, we introduce the Variable Compactness parameter per cluster that considers the geometry of the objects, or in other words, the fuzziness in the spatial domain. This parameter captures different variances of the clusters in a non-linear way, and thus improves the robustness of the clustering process. The cluster affection is done by an adaptive sequential forward floating selection (SFFS) approach that considers Zernike moments to maximize the intra-cluster similarity, which we consider as an originality and a main contribution in the proposed approach, illustrated in Fig. 1.

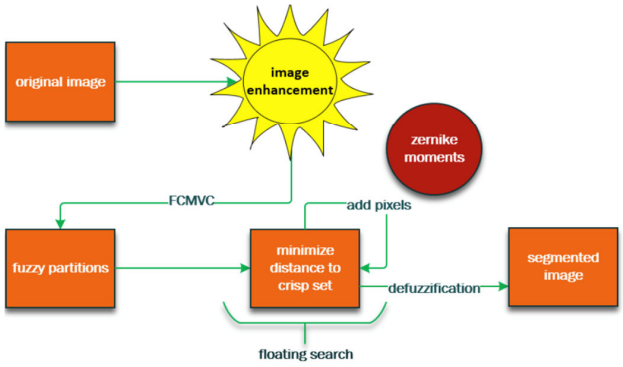

Fig. 1 Proposed approach

The paper is organized as follows: Section II depicts how image enhancement was conducted in the proposed approach; Section III talks about FCM and its variant with Variable Compactness; Section IV describes how defuzzification is performed by sequential forward floating selection with Zernike moments; results are shown in Section V; and the paper is concluded in Section VI.

II. Image Enhancement

The purpose of this process is to improve the interpretability of the information contained in the image for human viewers, or to provide a better input for some image processing process [6]-[8]. In this paper, two image enhancement techniques have been utilized: *Top-hat filtering* and *contrast stretching*.

The *top-hat filter* is defined as the residue of the original image and its opened version [2]. It is used to select objects that are darker (or brighter) than the local background for retention or removal. The top hat compares the darkest pixel in the inner region to the darkest pixel in the surrounding

Abder-Rahman Ali is with ISIT, Université d'Auvergne, UMR/CNRS/6284, BP10448, F-63000 Clermont-Ferrand, France (phone: 06-524-18395; e-mail: abder-rahman.ali@etu.udamail.fr).
Antoine Vacavant, Manuel Grand-Brochier, Adélaïde Albouy-Kissi, and Jean-Yves Boire are with ISIT, Université d'Auvergne, UMR/CNRS/6284, BP10448, F-63000 Clermont-Ferrand, France (e-mail: antoine.vacavant@udamail.fr, manuel.grandbrochier@udamail.fr, adelaide.kissi@udamail.fr, j-yves.boire@udamail.fr).

neighborhood. If the difference between those two pixels is greater than some threshold value, the pixel is kept, otherwise, it is not. This allows the selection of features based on size (defined by the inner region), contrast (the required difference in pixel values), and separation (width of the brim) [4].

Contrast stretching is a technique that enlarges the image's contrast, stretching the histogram to fill the full dynamic range of the image. With this technique, the histogram of an image would be expanded to cover all ranges of pixels [3], [5]. This technique improves the contrast of the image, such that it extends the intensity range of an image with a fixed ratio (highest pixel value / lowest pixel value) [5].

III. FCM with Variable Compactness

A. Fuzzy C-Means

Let $X=\{x_1,...,x_i,...,x_n\}$ be the set of n objects (*i.e.* set of pixels $f(x_1,y_1),\dots,f(x_i,y_i): i \in [1,\dots,m]\ and\ j \in [1,\dots,n]$, and $V=\{v_1,...,v_i,...,v_n\}$ be the set of c centroids in a p-dimensional feature space. Fuzzy C-Means partitions X into c clusters by minimizing the following objective function [1]:

$$J=\sum_{j=1}^{n}\sum_{i=1}^{c}\left(\mathbf{u}_{ij}\right)^{m}\left\|\mathbf{x}_j-\mathbf{v}_i\right\|^2 \tag{1}$$

where $1\le m\le\infty$ is the *fuzzifier*; $\mathbf{v}_j$ is the i^{th} centroid corresponding to cluster β_i; $\mathbf{u}_{ij}\in[0,1]$ is the fuzzy membership of the pattern $\mathbf{x}_j$ to cluster β_i; and $\|.\|$ is the distance norm such that,

$$\mathbf{v}_i=\frac{1}{n_i}\sum_{j=1}^{n}\left(\mathbf{u}_{ij}\right)^{m}\mathbf{x}_j \text{ where } n_i=\sum_{j=1}^{n}\left(\mathbf{u}_{ij}\right)^{m} \tag{2}$$

and,

$$\mathbf{u}_{ij}=\frac{1}{\sum_{k=1}^{c}\left(\frac{d_{ij}}{d_{kj}}\right)^{\frac{2}{m-1}}} \text{ where } d_{ij}^{\,2}=\left\|\mathbf{x}_j-\mathbf{v}_i\right\|^2 \tag{3}$$

FCM starts by randomly choosing c objects as centroids (means) of the c clusters. Memberships are calculated based on the relative distance (*e.g.* Euclidean distance) of the object $\mathbf{x}_j$ to the centroids using (3). After the memberships of all objects have been found, the centroids of the clusters are calculated using (2). The process stops when the centroids from the previous iteration are identical to those generated in the current iteration [1].

B. FCM with Variable Compactness (FCMVC)

FCMVC [6] is an enhancement to FCM, where a new geometric shape descriptor, the *compactness* $p_i, i=1,...,c$, is introduced, which captures different variances of the clusters (*i.e.* captures additional information of the underlying clusters), and thus, provides better clustering quality. The minimization (energy) function thus becomes as [6]:

$$J_{FCMVC}=\sum_{j=1}^{n}\sum_{i=1}^{c}\overline{\mu}_{ji}^{\,2}\left(\mathbf{x}_j-\mathbf{v}_i\right)^{2p_i} \tag{4}$$

The membership function now becomes:

$$\overline{\mu}_{ji}=\frac{\left(\mathbf{x}_j-\mathbf{v}_i\right)^{-2p_i}}{\sum_{i=1}^{c}\left(\mathbf{x}_j-\mathbf{v}_i\right)^{-2p_i}} \tag{5}$$

As p_i decreases, memberships increase for a fixed $\left|\mathbf{x}_j-\mathbf{v}_i\right|$. This implies that p_i is a measure of compactness of cluster i. The variable compactness parameter is chosen to be large for small classes and small for large classes [6].

IV. Defuzzification by SFFS and Zernike Moments

In fuzzy clustering, the minimization of the functional J, given in (1), leads to partitions characterized by the membership degree matrix. A *defuzzification* is thus needed to obtain the final segmentation. Usually, the data is attributed to the class having the highest membership degree. In medical imaging, this method does not give appropriate results because lesion borders are often not clearly defined.

The key point of this step is the calculation of the optimum threshold of the membership degree to obtain a consistent segmentation. For this purpose, we have introduced in [10] a novel defuzzification approach that considers two sets: the *support* (a crisp set of pixels having positive memberships) and the *core* (a crisp set with pixels having a membership equals to *1* which are certainly inside the object). A Sequential Forward Floating Selection (SFFS) procedure was then performed. This procedure is an iterative region growing approach. It is a bottom-up search procedure, where new pixels from the support set are added through applying Sequential Forward Selection (SFS), by starting from the core set, followed by a series of successive conditional exclusions of the worst feature in the newly updated set [7]. For conditional exclusions, Zernike moments [8] were employed as we will see below.

A. Zernike Moments

Moment descriptors have been studied for image recognition and computer vision since the 1960s [13]. The use of Zernike moments to overcome the shortcomings of information redundancy present in geometric moments was first introduced by Teague [14] [16].

Zernike moments are orthogonal moments (*i.e.* no redundancy or overlapping of information exist between the moments) based on Zernike polynomials. They are the mappings of an image onto a set of Zernike polynomials [17]. What distinguishes Zernike moments is the invariance of their magnitude with respect to rotation (*i.e.* independent of the rotation angle of the object), and can thus be utilized in describing the shape characteristics of objects [9], [17]-[18].

Given the ordered pair (m,n) that represent the Zernike polynomial order and the multiplicity (*i.e.* repetition) of its phase angle, the Zernike moment can be defined as follows [9]:

$$V_{nm}(\rho,\theta) = R_{nm}(\rho)e^{im\theta}, \theta \le 1 \quad (6)$$

such that,

$$\rho = \sqrt{x^2+y^2}, \theta = \arctan\left(\frac{y}{x}\right) \quad (7)$$

are the image pixel radial vector and angle between that vector and the X-axis, respectively.

The term R_{nm} shown in the following equation is the Zernike polynomial.

$$R_{nm}(\rho) = \sum_{a=0}^{\frac{(n-|m|)}{2}} (-1)^a \frac{(n-a)!}{a!\left(\frac{n+|m|}{2}-a\right)!\left(\frac{n-|m|}{2}-a\right)!}\rho^{n-2a} \quad (8)$$

The Zernike moment Z_{nm} for an image $\{f(x_i,y_i): 1 \le i \le M, 1 \le j \le N\}$ can be calculated as [9]:

$$Z_{nm} = \frac{n+1}{\pi}\sum_{i=1}^{M}\sum_{j=1}^{N} V_{nm}^{*}(x_i,y_j) f(x_i,y_j) \quad (9)$$

where $m = 0,1,2,3,...,\infty$ is the order of the Zernike polynomial; n is the multiplicity of the phase angles in the Zernike moment; and $x^2+y^2 \le 1$.

B. SFFS and Zernike Moments

The major contribution of this paper lies in embedding Zernike moments in SFFS for the conditional exclusion process, used as the defuzzification (*i.e.* decision) stage. As described in the previous section, since Zernike moments are independent of the rotation angle of the object, they are useful in describing the shape characteristics of the object (*i.e.* tumor). The pseudo-code for this proposed approach can be depicted as shown in Algorithm.1.

Notice that in order for a pixel *p* to be added to the crisp set, it has to meet the following criteria: (i) be a 4-neighbourhood of the crisp set (*i.e.* core); (ii) belongs to the support of the fuzzy set, but not to the crisp set; and (iii) minimizes the Zernike moment difference between the fuzzy set and the crisp set. This defuzzification approach overcomes the drawback inherent in defuzzification by α-cut (*i.e.* a crisp closed interval that contains only those points having a membership degree $\mu \ge \propto; \propto \in [0,1]$, where information is tend to be lost, and thus, unable to grasp the sense of uncertainty. It also takes into account the spatial relationships (*i.e.* 4-neighbors of a pixel p).

Algorithm 1: Defuzzification with Zernike moments

Input *grayscale image I*
apply top-hat filter and contrast stretch the image;
call *FCMVC on I /* parameters passed in this step are: input image, centroids, exponent (variable compactness), spatial smoothness, intensity threshold, and maximum number of iterations*/;*
fuzzySet ← I;
membershipMatrix ← μ; / μ is the degree of membership */*
core ← h(FuzzySet); / highest non-empty α-cut */*
n ← area(support(FuzzySet)) – area(core (FuzzySet));
C_0 = core(FuzzySet); / starting configuration */*
for *i ← 1…n* **do**
Ci ← [ ]; / empty set */*
end for
k ← 0;
minimum ← initial value; / temporary initial value, set as minimum */*
while *k < n* **do**
among the pixels p being 4-neighbor of C_k and not in $C_{k,,}$ and in support(FuzzySet):
/ select the pixel p that minimizes the Zernike moment difference between the FuzzySet and the CrispSet */*
find the Zernike moment of both the fuzzy set and the crisp set;
diff = |ZernikeMoment(FuzzySet) – ZernikeMoment(CrispSet)|;
if *diff < minimum*
minimum = diff; P={p};
else
P={ϕ};
end if
$C_{new} \leftarrow C_k \cup P$; $C_{k+1} \leftarrow C_{new;}$ k ← k+1;
end while

V. Results and Discussion

The performance of the proposed approach was tested on both synthetic images and medical images. We have studied five observation criteria [19], thereby highlighting the improvements in the segmentation, in terms of precision, shape, and information extracted. We relied on *precision*, *recall*, and the *Dice index*, all three defining statistically the quality of segmentation. We also analyzed the *Hamming measure*, which characterizes the number of disparities. Finally, the shape analysis was based on the determination of the *mean absolute distance* (denoted by MAD).

Precision and *recall* are defined as:

$$\text{Precision} = \frac{TP}{TP+FP} \quad (10)$$

$$\text{Recall} = \frac{TP}{TP+FN} \quad (11)$$

The *Dice index* is defined as:

$$\text{Dice index} = 2 \times \frac{Precision \times Recall}{Precision + Recall} \quad (12)$$

Hamming measure is defined as:

$$M_H(I_1 \Rightarrow I_2) = \text{n} - \sum_{R_2 \in I_2} max_{R_1 \in I_1} |R_2 \cap R_1| \quad (13)$$

where R_1 and R_2 are segmentation areas in the images I_1 and I_2, respectively. And, n is the number of pixels of one image.

The *mean absolute distance (MAD)*, which analyzes the contour points, and thus, the shape of the segmentation, is defined as:

$$\mathrm{MAD}(R_1, R_2) = \frac{1}{M}\sum_{m=1}^{M}\|x_m - y_m\| \quad (14)$$

where x_m and y_m are contour points of R_1 and R_2, respectively.

The parameters used with FCMVC were as follows: two *clusters* (*i.e.* object or tumor and background), which is the number of initial centroids (*i.e.* two centroids), set to 0 and 255, respectively, that is, [0,255]; *exponent* (*variable compactness*), a $c \times 1$ vector, where c is the number of clusters, was set to [1 1]; *spatial (membership) smoothness* [12] set to 0; *intensity threshold* (*i.e.* any intensity value in the image equal or below this value is considered a background) set to 0; and *maximum number of iterations* set to 20. The Zernike moment used was of degree (*i.e.* order) "4", and repetition "2".

A. Results with Synthetic Images

Four synthetic images were extracted from the database (D1)[1], which is composed of synthetic images with textured and uniform regions. The database includes 8400 images. Images used in the study were specifically extracted from the $B0U$ group, which consists of 100% textured regions. Images with 2-textures have been used in this study. Table I shows the numerical results obtained for our approach, and Fig. 2 illustrates them visually.

In view of the results presented in Table I, we can conclude that on such types of images, our approach provides good performance. Segmentations obtained are accurate, as shown by the index of Dice (close to 100%), their shape is consistent with the ground truth and the extracted information is reliable (just few disparities). It is important to note here that the image enhancement step of the proposed approach was not required for the synthetic images.

B. Results with Medical Images

Fig. 5 demonstrates how we construct our dataset from the original MR images: They are first annotated by a medical doctor (Figs. 3 and 4 show the original MR image and the medical doctor's annotations, respectively) so that we keep a ROI around the selected tumor. In this figure, a comparison between the proposed method with both the graph-cut and watershed approaches is also demonstrated. As can be noticed, the proposed approach provides a fine segmentation, as opposed to the other two approaches, where larger segments are obtained.

In order to apply our method on a concrete case, we studied its performance to segment liver tumors within MR images. The approach was applied on 8 cropped portions (ROIs) of MR liver tumor images. We show the results of four of these images, through Table II and Fig. 6.

TABLE I
NUMERICAL RESULTS FOR SYNTHETIC IMAGES

	B0U2R_2	B0U2R_7	B0U2R_54	B0U2R_56
Precision	99.97%	99.99%	99.85%	99.99%
Recall	99.19%	99.28%	99.21%	98.31%
Dice index	99.58%	99.64%	99.53%	99.15%
Hamming measure	444	388	502	901
MAD	1.18 pix.	0.97 pix.	2.01 pix.	3.65 pix.

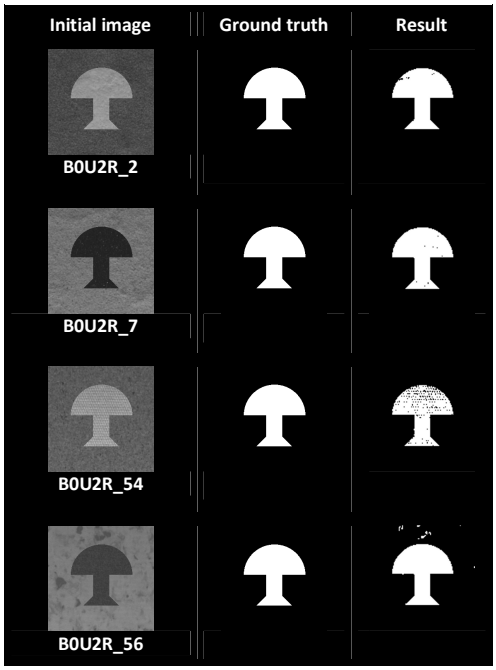

Fig. 2 Visual results for synthetic images

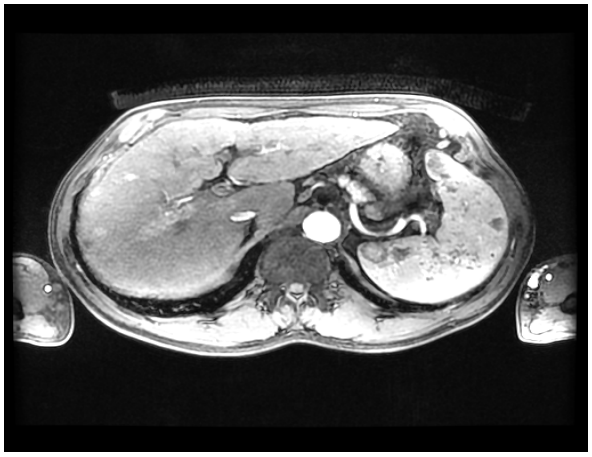

Fig. 3 Original MR image of Figs. 4, 5

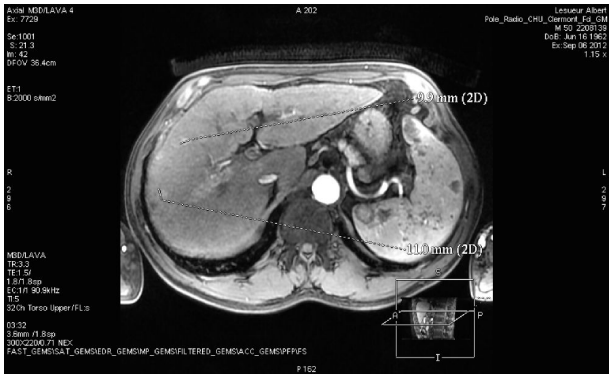

Fig. 4 Two tumor annotations of Figs. 3, 5

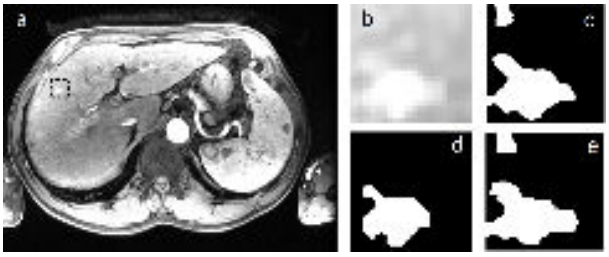

Fig. 5 (a) Original MR image with tumor of interest; (b) Cropped tumor (ROI); (c) Graph-cut approach result; (d)Proposed approach result; and (e) Watershed approach result

The results obtained on MR images confirm the observations of those in the previous subsection. (*A*) . Our approach allows, even for difficult cases such as MRI_2 or MRI_3, to extract a segmentation with good performance in terms of accuracy and shape, which implies that the geometry of the tumor is preserved for further clinical activities (such as automatic extraction of pharmaco-kinetics properties, lesion characterization, etc.).

TABLE II
NUMERICAL RESULTS FOR MEDICAL IMAGES

	MRI_1	MRI_2	MRI_3	MRI_4
Precision	97.63%	97.77%	93.23%	95.86%
Recall	99.75%	96.50%	99.60%	99.96%
Dice index	98.68%	97.13%	96.31%	97.87%
Hamming measure	379	783	1064	606
MAD	2.19 pix.	4.18 pix.	5.17 pix.	3.47 pix.

VI. CONCLUSION

The originality of the proposed approach lies in embedding Zernike moments within sequential forward floating selection for conditional exclusion, which aids in the decision (defuzzification) step in a fuzzy methodology. The approach provided an interesting performance. Results of the synthetic images were accurate (*i.e.* index of Dice close to 100%), their shape was consistent with the ground truth, and the extracted information was reliable (just few disparities). Results obtained on MRI images confirm such observations. Our approach allows, even for difficult cases of MRI images, to extract a segmentation with good performance in terms of accuracy and shape. In future studies, we aim at expanding this approach to work with synthetic images having more complex textures and to improve it for very difficult cases of liver tumor extraction.

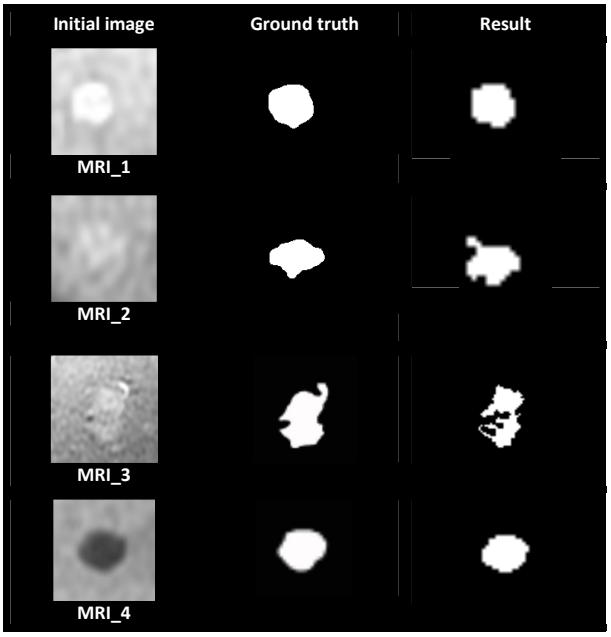

Fig. 6 Visual results for medical images

REFERENCES

[1] P. Maji and S. Pal. "Maximum Class Separability for Rough-Fuzzy C-Means Based Brain MR Image Segmentation," *T. Rough Sets*, Vol.9, pp.114-134, 2008.
[2] "Mathematical Morphology," (accessed May, 17 2015) http://www.cs.uu.nl/docs/vakken/ibv/reader/chapter6.pdf
[3] R. Crane, "Simplified Approach to Image Processing," Prentice Hall, 1997.
[4] J. Russ, "Image Analysis of Food Microstructure," CRC Press, 2004.
[5] J. Kim, "Image Enhancement for Improving Object Recognition," Algorithm and SoC Design for Automotive Vision Systems, Springer, 2014.
[6] S. Roy, H. K. Agarwal, A. Carass, Y. Bai, D. L. Pham, J. L. Prince, "Fuzzy C-Means with Variable Compactness," IEEE International Symposium on Biomedical Imaging, pp. 452-455, 2008.
[7] P. Pudil, J. Novovičová, J. Kittler, "Floating Search Methods in Feature Selection," Pattern Recognition Letters, volume 15, pages 1119-1125, 1994.
[8] A. Khotanzan, Y. H. Hong, "Invariant Image Recognition by Zernike Moments," IEEE Trans. PAMI, 12:489–497, 1990.
[9] B. Oluleye, A. Leisa, J. Leng, D. Dean, "Zernike Moments and Genetic Algorithm: Tutorial and Application," British Journal of Mathematics & Computer Science 4(15): 2217-2236, 2014.
[10] A. Ali, A. Albouy-Kissi, A. Vacavant, M. Grand-brochier, J. Boire, "A Novel Fuzzy C-Means Based Defuzzification Approach with an Adapted Minkowski Distance," 19th Computer Vision Winter Workshop Zuzana Kúkelová and Jan Heller (eds.) Křtiny, Czech Republic, 2014.
[11] R. Fang, R. Zabih, A. Raj, T. Chen, "Segmentation of Liver Tumor Using Efficient Global Optimal Tree Metrics Graph Cuts," In Abdominal Imaging. Computational and Clinical Applications, 2012.
[12] D. Pham, "Robust Fuzzy Segmentation of Magnetic Resonance Images, 14th IEEE Symposium on Computer-Based Medical Systems, p. 127-131, 2001.

[13] C. Teh and R.T. Chin, “On Image Analysis by the Methods of Moments,” IEEE Trans. on PAMI, 10 (4). 496-513, 1988.
[14] M. Teague, “Image Analysis via the General Theory of Moments,” Journal of the Optical Society of America, 70 (8). 920-930, 1980.
[15] J.S. Lipscomb, “A Trainable Gesture Recognizer,” Pattern Recognition, 24 (9). 895-907, 1991.
[16] H. Hse and A. Newton, “Sketched Symbol Recognition Using Zernike Moments,” In Proceedings of ICPR, 2004.
[17] A. Tahmasbi, F. Saki, and S. B. Shokouhi, "Classification of Benign and Malignant Masses Based on Zernike Moments," J. Computers in Biology and Medicine, vol. 41, no. 8, pp. 726-735, 2011.
[18] A. Tahmasbi, F. Saki, H. Aghapanah, and S. B. Shokouhi, "A Novel Breast Mass Diagnosis System based on Zernike Moments as Shape and Density Descriptors," In Proc. IEEE, 18th Iranian Conf. on Biomedical Engineering (ICBME'2011), Tehran, Iran, pp. 100-104, 2011.
[19] M. Grand-Brochier, A. Vacavant, G. Cerutti, K. Bianchi, and L. Tougne, “Comparative Study of Segmentation Methods for Tree Leaves Extraction,” In ACM ICVS 2013, Workshop: VIGTA, Saint Petersburg, Russia, 2013.